

Summary of Professional Accomplishments

1. Name

Johannes Robert Binder

2. Diplomas, degrees conferred in specific areas of science or arts, including the name of the institution which conferred the degree, year of degree conferment, title of the PhD dissertation

2015 – **PhD degree in physics** (with distinction) awarded by the Faculty of Physics, University of Warsaw. Title of the PhD thesis: „Carbon based nanostructures for detectors and biosensors”, supervisor: prof. Andrzej Wyszomolek, co-supervisor: dr. Marta Borysiewicz

2010 – “**Diplom-Physiker**” (**MSc**) awarded by the University of Tübingen, Germany, supervisor: prof. Dieter Kern. Title of the MSc thesis: „Electron source with carbon nanotubes as field emitters”

3. Information on employment in research institutes or faculties/departments or school of arts.

June 2016 – present: **adiunkt (research and teaching position)** at the Faculty of Physics, University of Warsaw

May 2015 - April 2016: **post-doc position** at the National High Magnetic Field Laboratory, Grenoble, France (group of prof. Marek Potemski)

4. Description of the achievements, set out in art. 219 para 1 point 2 of the Act

The achievement described in this paragraph is based on a series of publications addressing the topic of “**Physical effects at interfaces between and within layered materials**”. The series consists of the following six scientific publications:

[H1] **J. Binder**, F. Withers, M.R. Molas, C. Faugeras, K. Nogajewski, K. Watanabe, T. Taniguchi, A. Kozikov, A.K. Geim, K.S. Novoselov, M. Potemski “*Sub-bandgap Voltage Electroluminescence and Magneto-oscillations in a WSe₂ Light-Emitting van der Waals Heterostructure*” *Nano Letters* 17, 1425-1430 (2017)

I carried out the optoelectronic measurements, analysed and interpreted experimental data, participated in discussions, developed the model, and wrote the draft of the publication. I am also a corresponding author of this work.

[H2] **J. Binder**, J. Howarth, F. Withers, M.R. Molas, T. Taniguchi, K. Watanabe, C. Faugeras, A. Wymolek, M. Danovich, V.I. Fal'ko, A.K. Geim, K.S. Novoselov, M. Potemski, A. Kozikov "Upconverted electroluminescence via Auger scattering of interlayer excitons in van der Waals heterostructures" *Nature Communications* 10, 2335 (2019)

I carried out the optoelectronic measurements, analysed and interpreted experimental data, participated in discussions, developed the model, and wrote the draft of the manuscript.

[H3] **J. Binder**, J. Rogoza, L. Tkachenko, I. Pasternak, J. Sitek, W. Strupinski, M. Zdrojek, J.M. Baranowski, R. Stepniewski, A. Wymolek "Suspended graphene on germanium: Selective local etching via laser-induced photocorrosion of germanium" *2D Materials* 8, 035043 (2021)

I conceived and carried out the experiments, analysed the data and developed a model to explain the observations. I wrote the draft of the publication and a patent application. I am also the corresponding author of this work.

[H4] **J. Binder**, A. K. Dabrowska, M. Tokarczyk, K. Ludwiczak, R. Bozek, G. Kowalski, R. Stepniewski, and A. Wymolek "Epitaxial hexagonal boron nitride for hydrogen generation by radiolysis of interfacial water" *Nano Letters* 23, 1267–1272 (2023)

I performed the scanning electron microscope imaging and irradiation, carried out the optical measurements, interpreted the results, conceived the experiment with heavy water and wrote the draft of the manuscript. I am also the corresponding author of this work.

[H5] K. Ludwiczak, E. Lacinska, **J. Binder**, I. Lutsyk, M. Rogala, P. Dabrowski, Z. Klusek, R. Stepniewski, A. Wymolek "Impeded phase transition in 1T-TaS₂: Thermoelectric fingerprint of long-lived mixed states" *Solid State Communications* 305, 113749 (2020)

I participated in the optical and optoelectronic measurements, supervised the bachelor student and co-supervised the PhD student, proposed and developed the experimental setup, interpreted the data and participated in the writing of the manuscript. I am also the corresponding author of this work.

[H6] E. M. Lacinska, M. Furman, **J. Binder**, I. Lutsyk, P. J. Kowalczyk, R. Stepniewski, A. Wymolek "Raman Optical Activity of 1T-TaS₂" *Nano Letters*, 22, 2835 – 2842 (2022)

I participated in the optical measurements, co-supervised the PhD student, participated in developing the experimental setup, interpreted data and participated in the writing of the manuscript.

The series of publications presented above comprises results which all address the fundamental research question of physical effects between interfaces of layered (or in the few-layer limit – of two-dimensional (2D)) materials with other materials (2D materials, conventional bulk semiconductors, liquids and gases) and ‘interfaces’ occurring within a single layered material that can host different phases at the same time. The knowledge obtained is of major importance both from a fundamental scientific point of view, but also for future possible applications based on the novel concept of van der Waals (vdW) heterostructures [1]. It is clear that especially 2D materials, due to their reduced dimensionality, are prone to the physical properties of their surrounding and only a deep understanding of the major effects occurring at interfaces allows to study novel physical phenomena and develop new optoelectronic device concepts.

1. Interfaces of 2D materials with other 2D materials ([H1] and [H2])

The first part of my research was devoted to interfaces of 2D materials with other 2D materials. Such structures are called van der Waals (vdW) heterostructures. Due to the lack of covalent bonds out-of-plane, it becomes possible to stack materials of different type (metal, semiconductor, insulator) with different lattice constants, opening up new possibilities of optoelectronic device construction [1]. An example of such a class of devices are light-emitting diodes based on vdW heterostructures [2], which I studied in works [H1] and [H2].

Figure 1 (a) presents a microscope image showing a stack of 2D layers and Figure 1 (b) shows a schematic drawing of the structure used in the work [H1]. The sample was fabricated by mechanical exfoliation of layered materials to obtain flakes of single- or few-layer thickness that are subsequently stacked on top of each other. The fabrication process was performed in the group of Nobel prize laureate, Prof. Konstantin Novoselov at the University of Manchester. This sample consisted of a monolayer (ML) of WSe₂, which is a semiconducting transition-metal dichalcogenide (TMD) with a direct bandgap, sandwiched from both sides by hexagonal boron nitride (hBN) and monolayer graphene electrodes. Figure 1 (c) shows the differential conductance of this structure upon application of a voltage between the two graphene electrodes. The strong increase in conductance at about 1.7 V corresponds to a strong increase in measured electroluminescence (EL) (Fig. 1 (d)).

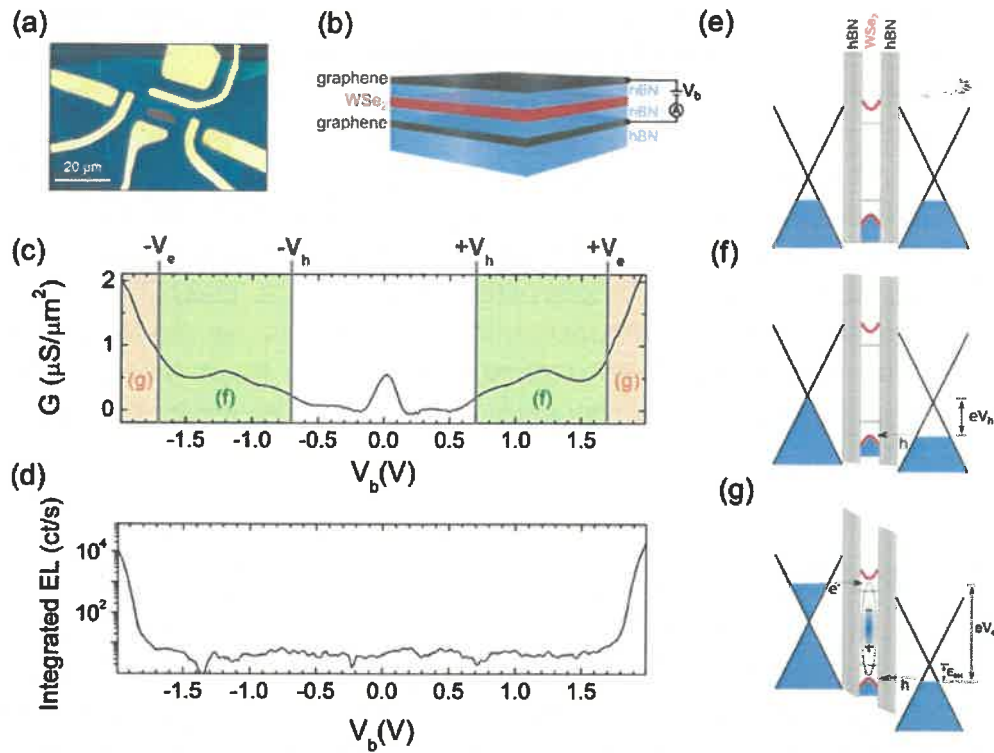


Figure 1: (a) Optical microscope image of the sample. The brown area indicates the WSe₂ flake. (b) Schematic illustration of the vdW heterostructure. (c) Differential conductance $G = dI/dV_b$ (d) EL signal as a function of the bias voltage. (e) Schematic band diagram for zero bias. (f) Schematic band diagram for the case of intermediate bias. (g) Band diagram for large bias. In this case, both holes and electrons can tunnel and directly form excitons.

Figures 1 (e)-(g) depict the actual mechanism that leads to the observed current flow. It is clear that the observed current is due to charge carrier tunnelling across the interfaces between 2D materials. An EL onset voltage of about 1.7 V can be extracted, which fits the energy of the excitonic transition of the monolayer WSe₂. However, the band gap of ML WSe₂ (~2.0 - 2.2 eV) [3, 4] is much larger than the voltage onset. The difference is given by the large exciton binding energy in ML WSe₂. The clear onset of EL for voltages of about 1.7 V means that tunnelling occurs directly into the excitonic state and not via electrons (holes) that are first injected into the conduction (valence) band, which would require voltages above 2 V. Note that the measurements were performed at T=4 K. Our research hence revealed the process of sub-bandgap voltage emission in light-emitting vdW heterostructures.

An additional observation governed by charge transfer across the 2D material / 2D material interface is depicted in Figure 2 (a). It shows the dependence of the EL as a function of magnetic field. Clear magneto-oscillations are apparent, with a periodicity of $1/B$. The interpretation of these oscillations is given in Figure 2 (b). Upon application of the magnetic field, the density of states (DOS) in the graphene electrodes consist of Landau levels. This quantized DOS now leads to oscillations of the tunnelling probability from graphene into the light emitting WSe₂ layer, which can be directly observed as oscillations in the EL intensity. The fingerprint of graphene in this modulation is the square-root dependence of the energy of the Landau levels with magnetic field [H1].

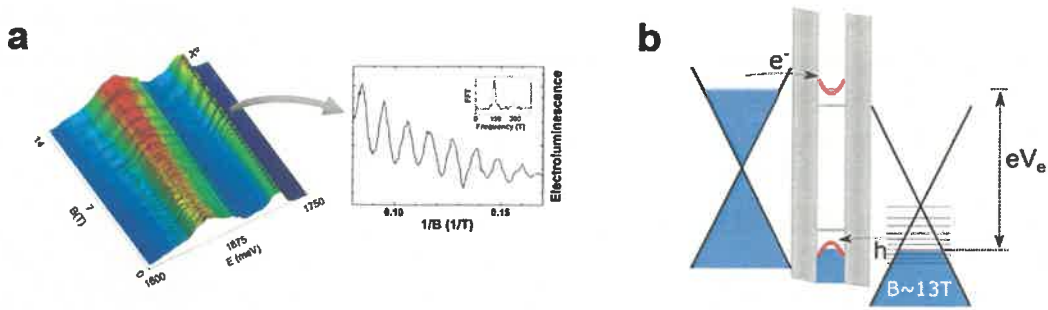


Figure 2: (a) 3D false colour plot of the EL signal as a function of the magnetic field. *Inset:* Intensity of the neutral exciton as a function of $1/B$. (b) Schematic illustration of the Landau quantization in the graphene electrode leading to magneto-oscillations.

In the work [H2], the studied vdW heterostructures are more complex featuring two different TMD ML (MoS_2 and WSe_2), see Figure 3 (c,d). This structure is asymmetric and has a type-II band alignment (Fig. 3 (b)). In structures of this type, indirect, interlayer excitons are expected to be formed when charge carriers are injected electronically. Most importantly, such transitions are not only indirect in real space (with electrons in MoS_2 and holes in WSe_2), but also indirect in momentum space. This momentum mismatch can be divided into two contributions, which are shown in Fig. 3 (a). First, MoS_2 and WSe_2 have a lattice mismatch of about 4 %. Second, a misorientation of the layers (twist angle) leads to an additional mismatch.

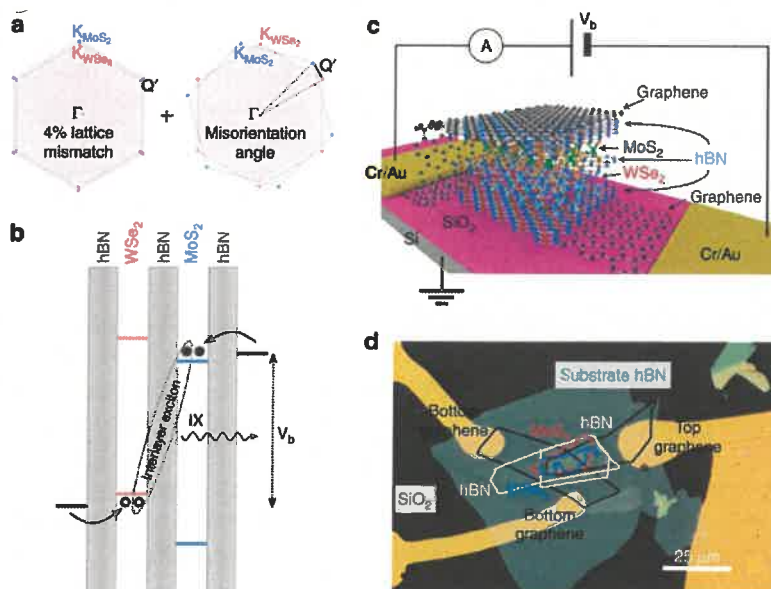


Figure 3: (a) Brillouin zones of WSe_2 (red) and MoS_2 (blue) illustrating the momentum Q' arising from the lattice mismatch and misorientation angle. (b) Schematic illustration of the type-II band alignment for the $\text{MoS}_2/\text{WSe}_2$ heterostructures. The dashed ellipse indicates the formation of an interlayer exciton consisting of an electron in the conduction band of MoS_2 and a hole in the valence band of WSe_2 . (c) Schematic drawing of the heterostructure shown in (b). (d) Optical microscope image of the active area of the device.

In publication [H2] I studied seven devices based on vdW structures, of which five had a hBN spacer between the TMDs and two did not have a spacer. For the devices without the spacer, a typical behaviour of EL emission with applied voltage was observed, which is a step-like appearance according to larger energies of the excitonic resonances. First an emission of the indirect exciton (IX) is observed; then we observe emission of WSe₂ for voltages of about 1.75 V and 2.1 V in the case of MoS₂ (Fig. 4 (a-b)). The emission of the IX blueshifts with increasing voltage, which is a consequence of the electric field that builds up between the two TMDs and a fingerprint of indirect excitons. The IX emission is hence tuneable with a slope in the range of 90 - 200 meV/V. From the behaviour of the IX emission I could also estimate the interface bandgap between MoS₂ and WSe₂ to be around 1.08 eV (inset Fig. 4 (b)).

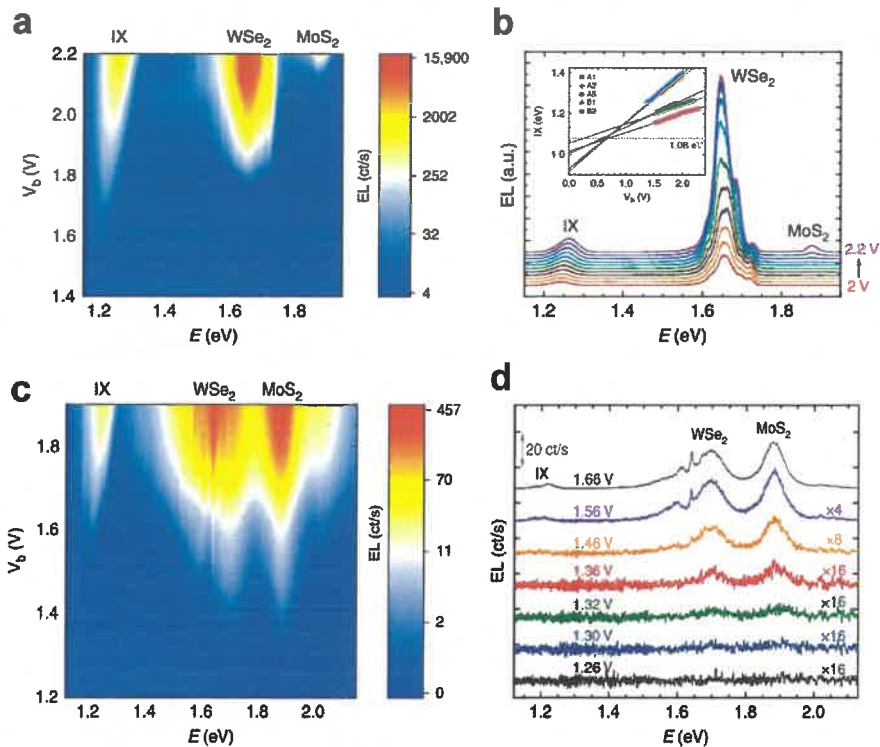


Figure 4: (a) False colour contour plot of the EL spectra as a function of the bias voltage. (b) EL spectra for biases in the range of $V_b = 2.0 - 2.2$ V extracted from (a). The spectra are vertically shifted for clarity. The inset in panel (b) shows the peak position of the IX as a function of bias for five different samples and linear fits to the dependencies. (c) False colour contour plot of the EL spectra as a function of bias voltage for a sample with a monolayer hBN spacer. (d) EL spectra for seven different bias voltages extracted from (a). The spectra are vertically shifted for clarity. For a voltage of $V_b = 1.32$ V emission at energies up to around 1.9 eV are observed, clearly illustrating the large upconversion effect.

The situation changes for samples with a monolayer hBN spacer between the TMDs. Figures 4 (c,d) show that now the emission related to WSe₂ (~1.7 eV) and MoS₂ (~1.9 eV) appear for voltages as low as around 1.3 V, which constitutes a remarkable electroluminescence upconversion of ~ 0.6 eV. The physical mechanism behind this observation is illustrated in Figure 5. The indirect nature of the IX corresponds to a momentum mismatch (Q') as indicated in this two-particle picture. As a consequence

of the low injection barrier, IX are formed in large numbers. Due to the momentum mismatch, they are not in the light cone and cannot effectively recombine radiatively. Thus, further electrical pumping creates large populations of IX that may lead to radiative recombination (I) if IX reach a momentum of Q' . However, this channel is very ineffective. A further increase of the IX population gives rise to effective nonradiative recombination via IX-IX collisions. In such a process, the energy is transferred to another IX that is excited into the continuum of excitonic states (II). From this state, the exciton can either relax back in the IX state, which is called (i) exciton-exciton annihilation, or relax into a state that corresponds to either (ii) a MoS₂ or (iii) a WSe₂ intralayer exciton. Processes (ii) and (iii) are excitonic Auger processes that can explain the observed electrically-induced upconversion.

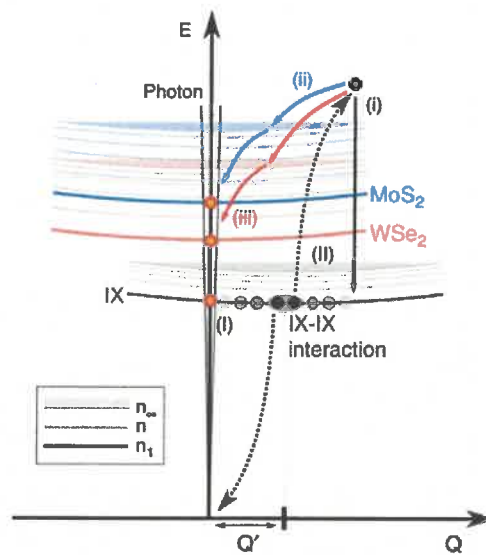


Figure 5: Mechanism of up-converted emission in the two-particle picture. The solid lines represent the excitonic ground-state dispersion n_1 of the IX (grey), MoS₂ (blue) and WSe₂ (red). The circles represent excitons. Q' is the momentum mismatch. The dashed lines indicate excited states n and the shaded area marks the excitonic continuum n_∞ . The greyscale shading of circles schematically shows the momentum distribution of excitons. The bright shading indicates that there are less excitons for a given momentum than for the dark shading. The photon dispersion is overlaid (grey lines) to mark the region of effective radiative recombination (orange circles). For the situation depicted, the bias voltage is below the threshold for direct intralayer charge injection. Mechanism (I) illustrates radiative IX emission facilitated by an increasing number of IX with large momenta. Mechanism (II) depicts excitonic Auger processes. The grey ellipse schematically highlights the interaction between the two exemplary excitons. As a result of the interaction, one exciton recombines nonradiatively and transfers the energy to the other exciton (arrows with dotted lines). Relaxation: (i) describes relaxation back to the IX ground state (exciton – exciton annihilation), (ii) and (iii) relaxation to MoS₂ and WSe₂, respectively, which leads to upconverted intralayer emission

The observed mechanism shows that large IX populations can be achieved in such structures, which is interesting in terms of a possible Bose-Einstein condensation. Moreover, we observe that the Auger effect effectively converts a part of the nonradiative recombination into radiative recombination taking place within the ML TMD layers. Hence, part of the otherwise lost emission is recaptured by this

mechanism, which may be an interesting aspect for future vdW light-emitting device engineering.

2. Interface of a 2D material with a bulk semiconductor [H3]

This part of my studies was dedicated to graphene on germanium, which is considered a prospective material for integration of graphene with silicon based technology [5]. The Raman spectrum of graphene grown on germanium is, however, known to be weak, which can be seen by the ratio of the Raman peaks of graphene on germanium to the peak of nitrogen in air ($\sim 2330\text{ cm}^{-1}$) presented in several publications [6, 7]. To answer the question whether these low Raman signals are inherent to graphene on germanium or are due to the interface of the 2D material with a bulk semiconductor, I developed a novel technique of locally removing germanium without damaging graphene [H3]. The etching process is facilitated by a photocorrosion mechanism that has previously been used for doped III-V semiconductors [8]. This photocorrosion process allows us to etch germanium in ultrapure, deionised water by exposing germanium to a conventional, focused cw-laser with a few milliwatts of power. Arbitrary structures can be etched into bulk germanium, for example, by using a conventional Raman spectroscopy setup. Scanning electron microscope (SEM) images of structures etched into bulk germanium are shown in Figure 6. A patent application that describes this selective etching process has been filed.

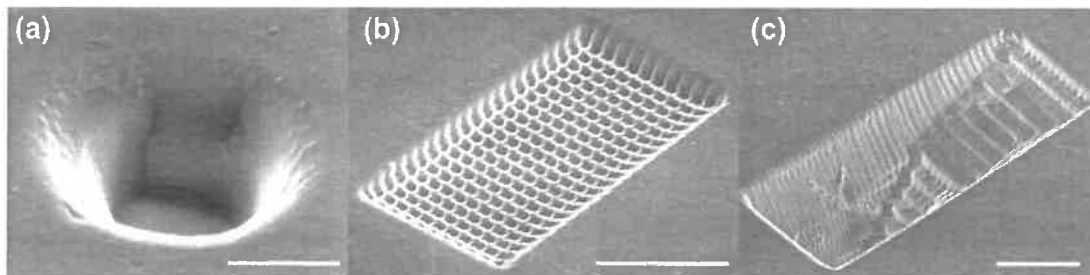


Figure 6: Scanning electron microscope images of photoetched bulk germanium. (a) Single point exposure resulting in submicrometre sized holes (scale bar: 400 nm). (b) Two-dimensional etch pattern obtained by moving the stage between the consecutive etch steps (scale bar: 4 μm). (c) Three-dimensional structures obtained by using different dwell times. The staircase-like structure obtained is about 10 μm deep (scale bar: 5 μm).

With this process, one can selectively underetch graphene, by removing solely the germanium underneath, as schematically shown in Figure 7 (a). This method allows us to compare pristine and suspended graphene on the same sample without any transfer or further etching. Figure 7 shows the results of the Raman (d-e) mapping of a freestanding graphene membrane shown in panel (b) and (c). An increase of the Raman signal by orders of magnitude is observed on the suspended graphene. Additional measurements performed in-situ during the actual etching process show a similar strong increase in the graphene signal [H3].

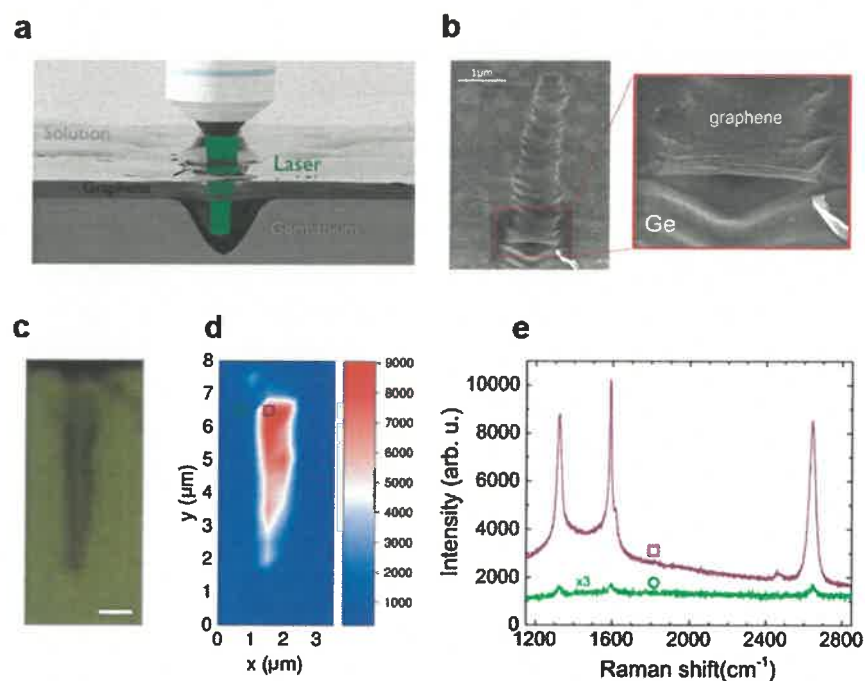


Figure 7: (a) 3D illustration of the setup used for the direct-writing etching process. (b) Scanning electron microscope cross section image of a free-standing graphene membrane. (c) Optical microscope image of the graphene membrane shown in figure (b). The scale bar is 1 μm . (d) False colour map showing the graphene 2D band peak intensity. The green circle and the purple square indicate the two positions for which the Raman spectra are presented in (e).

On the basis of these findings we can conclude that the low Raman signals of graphene on germanium are not related to its quality but are a consequence of the interaction between graphene and germanium at the interface. The Raman signal is quenched because the excitation is effectively transferred to the underlying germanium substrate that has a bandgap energy which is much lower than the photon energy of the lasers (1.96 eV, 2.33 eV) used for the Raman mapping.

3. Interface of a 2D material with liquids and gases [H4]

The third class of interfaces is related to a very common situation, which is a 2D material that is exposed to liquids or gases under ambient conditions. Especially, the role of water is crucial for 2D materials, even if they are stable under ambient conditions. The system that was used to study this influence is epitaxial hBN grown by metalorganic vapour-phase epitaxy (MOVPE) in our research group at the Faculty of Physics, University of Warsaw (Layered Materials Laboratory, prof. Andrzej Wyszomółek, prof. Roman Stępniewski). The material is grown at high temperatures above 1000 $^{\circ}\text{C}$ on sapphire substrates. Since hBN is a layered material, the growth of high quality hBN should lead to a layer that ideally has no covalent bonds with the substrate. Such a lack of covalent bonds is important to understand the behaviour of epitaxial hBN during the cooling process after growth. This situation is illustrated in Figure 8 (a). The hBN layer is unstrained at the growth temperature but upon cooling the sapphire substrate

shrinks and the hBN expands, as it has a negative in-plane thermal expansion coefficient [9]. Since the layer is weakly attached, the large resulting strain does not lead to cracks, but to the formation of wrinkles [10].

For such epitaxial hBN with wrinkles, we observed the formation of bubbles upon exposure to an electron beam inside a SEM during imaging (video available online as supplementary information to [H4]). This observation could be explained by electrostatic charging effects, as both sapphire and hBN are insulators, or by a reaction triggered by the electron beam. To gain further insight into the actual mechanism, we performed micro-Raman spectroscopy mapping of such a bubble; see Fig. 8 (b-d). A line scan across the bubble clearly shows the appearance of new Raman lines. These lines are only apparent for spots on the bubble and could be identified to be due to molecular hydrogen, as evidenced by five bands that fit the rovibrational spectrum of H_2 (Fig. 8 (d)) [11].

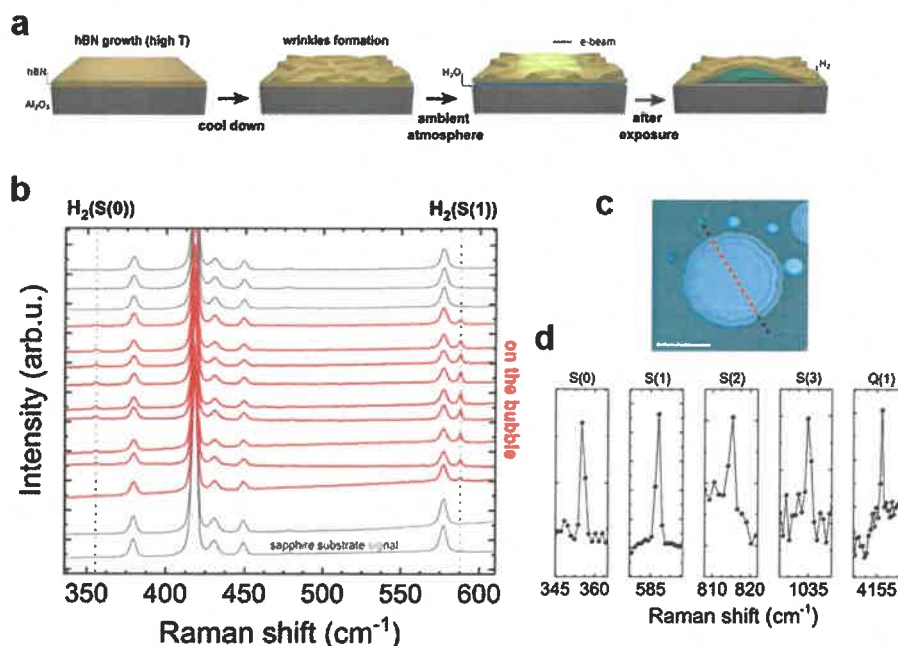


Figure 8: (a) Schematic illustration of bubble formation. hBN is grown by MOVPE at temperatures above 1000 ° C. After the growth, the sample was cooled to room temperature, which led to the formation of hBN wrinkles. The sample is removed from the reactor and exposed to ambient conditions. Exposure to an electron beam in a SEM leads to bubble formation. (b) Raman line scan across a hydrogen-filled bubble. It can be clearly seen that two lines are present on the bubble only. These lines correspond to the lines of molecular hydrogen. Raman spectra are shifted vertically for clarity. (c) Optical microscope image of the studied bubble showing the laser spot (532 nm). The dashed line indicates the direction of the line scan. (d) Additional rovibrational lines measured on the bubble not shown in the line scan. It was possible to identify the first four lines S(0)–S(3) of the (0–0) transitions and line Q(1) of the (1–0) transitions.

This conclusion raises the question regarding the source of the observed hydrogen. In principle, there are two possibilities: (1) H_2 either stems from hydrogen that is available during the growth, from the H_2 carrier gas or the precursor gases (NH_3 , TEB), or (2) is

introduced after the growth outside the reactor. To distinguish between these two possibilities, a control experiment was conceived using heavy water as spectroscopic marker. To this end, a sample was placed in a sealed container with heavy water. The sample was mounted upside down at the top of the container to avoid any direct contact with heavy water (Fig. 9 (a)). This way the sample was exposed to an atmosphere containing heavy water. After 23 days, the sample was removed from the container and transferred to the SEM to initiate bubble formation. After the successful creation of bubbles, the sample was studied by Raman spectroscopy. Figure 9 (a) shows the optical image of the bubble and two spots that mark the corresponding spectra shown in panel (b). Apart from the lines related to H_2 , a new set of lines appears which is related to hydrogen deuteride (HD), which is the diatomic compound of two isotopes of hydrogen (1H : protium and 2H : deuterium). Due to the low natural abundance of deuterium, we can claim the deuterium observed in HD stems from the heavy water. Therefore, one can conclude that at least part of the observed hydrogen comes from the intercalation of water occurring at the interface. Upon irradiation with an electron beam, radiolysis occurs, which leads to the dissociation of water and the generation of H_2 that is effectively stored at the interface inside the hBN bubbles. Bubble formation is further facilitated by the wrinkled surface of the layer. Bubble formation is one way to relax the layers and compensate for the strain accumulated in the wrinkles.

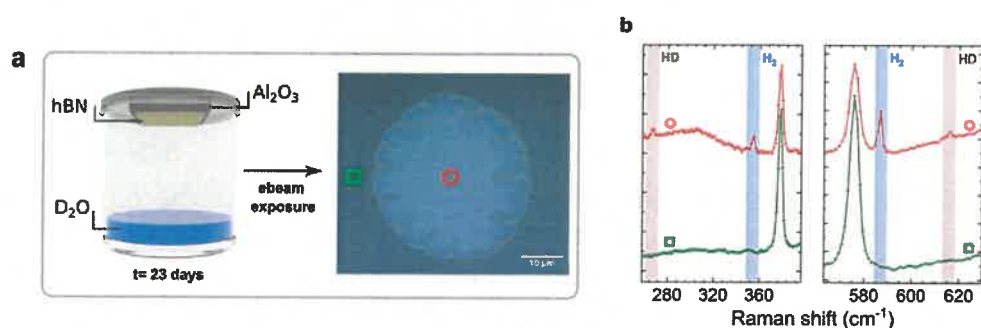


Figure 9 (a) The sample was mounted upside down in a container filled with heavy water (D_2O) for 23 days. Subsequently, the sample was directly mounted in the SEM and exposed by e-beam irradiation to form bubbles as shown in (a). (b) Raman spectra of two typical points on (next to) the bubble are shown as red (green) curves. The spectrum next to the bubble shows only Raman bands related to sapphire. For the measurement on the bubble, not only a signal related to molecular hydrogen, but also a signal related to hydrogen deuteride (HD) can be observed.

It has been already shown that a single layer of BN on one hand is an excellent proton conductor [12], but on the other hand an excellent barrier for H_2 [13, 14]. In our case of an epitaxial material, H_2 was measurable inside the bubble for more than 4 weeks. Afterwards, the signal vanished. Based on this observation, one can conclude that despite the presence of defects, our epitaxial hBN can possibly fulfil the role of hydrogen barrier, which opens up many possible applications, for example for lightweight H_2 tanks. However, it is not clear what mechanism causes the decrease in signal. After radiolysis, not only H_2 is formed, but also other reaction products, mostly H_2O_2 [15]. In our specific case, all reaction products remain confined inside the hBN

bubble. Therefore, back reactions might occur. Indeed, such back reactions are one of the main limiting factors of H₂ production by radiolysis in pure water in closed systems [15]. Therefore, it is difficult to assess if the H₂ escapes the hBN layer or vanishes due to back reactions. To be able to make any statement about the mechanical suitability of the epilayers for H₂ storage, we performed a mechanical stress test. To this end, we made use of the fact that the bubbles form in a SEM under vacuum. If the bubbles are removed from the SEM, the bubbles will be exposed to atmospheric pressure. For small bubbles almost no change is observed, but for large bubbles, the atmospheric pressure leads to a flattening of the bubble. Based on this effect, we performed an automated pressure cycle on a large bubble ($\approx 150 \mu\text{m} \times 200 \mu\text{m}$) that leads to an inflation and deflation of the bubble (video available online as supplementary information to [H4]). After a certain number of cycles, Raman spectroscopy was performed to assess if H₂ was still present in the bubble. Even after the maximum number of 551 cycles hydrogen was present in the bubble, which shows that our hBN remains leakproof even under extreme mechanical deformation.

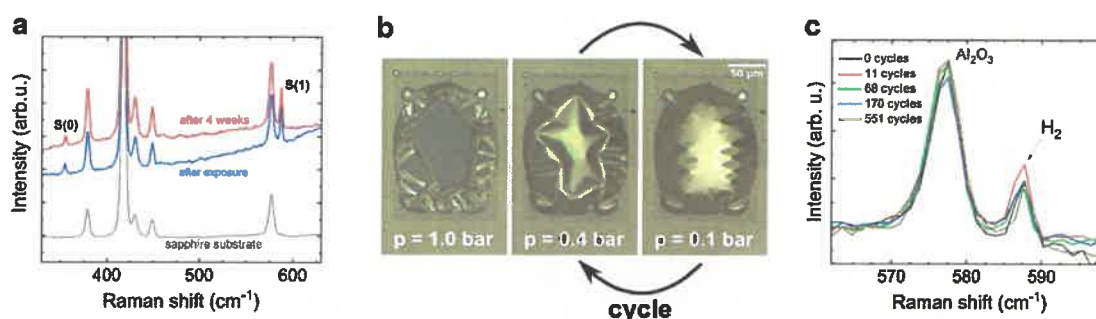


Figure 10: (a) Two Raman spectra taken at the same point of the bubble directly after exposure to the electron beam and after 4 weeks. The Raman lines did not decrease in intensity. This means that the hydrogen is still confined in the bubble after 1 month under ambient conditions. The Raman spectrum of a bare sapphire substrate is shown for comparison. (b) Optical microscope images of a large bubble for different ambient pressures. The bubble was inflated and deflated by automatically cycling the pressure between 100 and 400 mbar. (c) After certain number of pressure cycles Raman measurements were performed. Molecular hydrogen was still present after 551 cycles.

These findings show that hBN holds great prospects for applications in hydrogen storage and could allow for the development of unconventional hydrogen generation schemes by making use of chemical reactions happening in a nanoconfined space at the interface of hBN and other materials.

4. Interface within a 2D material that hosts different phases: [H5] and [H6]

This chapter addresses “interfaces” within a single layered material, namely the 1T polytype of tantalium disulfide (1T-TaS₂). This transition-metal dichalcogenide has been studied intensively for many decades and possesses a very rich phase diagram [16]. Several temperature-dependent phase transitions can be observed. With

decreasing temperature, 1T-TaS₂ undergoes a phase transition ($T = 550$ K) from a metal-like to an incommensurate charge density wave phase. At around 350 K another phase transition to a nearly commensurate charge density wave (NCCDW) phase takes place, followed by a transition to a commensurate charge density wave (CCDW) phase at a temperature of around 180 K. The charge density wave phases are accompanied by a periodic lattice distortion, for which the position of the atoms are shifted to form a Star-of-David-like pattern. These phase transitions have been studied in detail in recent decades using many different measurement techniques such as electron microscopy [17], scanning tunnelling microscopy [18, 19], optical spectroscopy [20], measurements of elastic properties [21] and electrical transport measurements [22]. A prominent feature of the electrical properties is a change from n-type (NCCDW) to p-type (CCDW) conductivity, which also results in a change in the sign of the Seebeck constant, which we used in our work [H5].

A simple observation of changes in resistance is one of the most straightforward methods for measuring the phase transition between the NCCDW and CCDW phases and is hence widely applied to study the system. However, this method has a global character as it probes the behaviour of the whole sample, not allowing us to study the phase transition with spatial resolution. During the phase transition one can observe spontaneous jumps in resistance, which might be attributed to phase transitions of parts of the sample. In such a situation, two phases should be present at the same time, separated by an interface or junction. Such a mixed phase of CCDW (p-type) and NCCDW (n-type) is very interesting, since a p-n junction should form at the interface between regions of different phases.

The aim of the work [H5] was to study such mixed states by optoelectronic measurements that allow to probe the sample locally with a focused laser spot (micro-Raman spectroscopy) and globally by measuring the electrical resistance. While performing these measurements we observed a strong impact of the electrical response upon irradiation with a focused laser beam. The current voltage curves of illuminated samples allowed us to conclude that the laser beam induces a heat gradient on the sample that results in a thermoelectric voltage (Seebeck effect). Since the laser can be moved with submicrometre precision, we obtained a tool to probe the properties of the sample by moving the laser, which acts as a local heat source on the sample. When the region close to a contact is illuminated, the carriers move to the opposite side thereby creating an additional voltage. The sign of this voltage will be inverted when the laser is placed close to the opposite contact. Generally, the sign of a thermoelectric voltage also depends on the type of majority carriers. Since the type of charge carriers changes during the phase transition, the Seebeck coefficient also changes and hence we obtain inverted signs of thermoelectric voltages. This behaviour can be observed by comparing Figure 11 (a) for the CCDW phase and (c) for the NCCDW phase. The sign of the induced voltage close to the contacts is inverted, which illustrates that our method works as expected. To study the mixed state, with interfaces between CCDW and NCCDW phases, we performed laser-induced thermoelectric voltage mapping during the phase transition. By observing the changes in resistance, we can follow the progress of the phase transition. We were able to show that mixed states can be stabilized by lowering the temperature (by about 3 K) in the course of an unfinished phase transition. A spatial map of the thermoelectric voltage for this

interrupted transition is shown in Figure 11 (b). One can see that the overall reaction is very distinct from the CCDW (Fig. 11 (a)) and NCCDW (Fig. 11 (c)) phases. Now we obtain a maximum of the thermoelectric voltage in the centre of the sample. We have shown that such states are stable for several hours, yielding the same result for consecutive thermoelectric voltage maps. By slightly increasing the temperature the phase transition continues, and a subsequent lowering of the temperature interrupts the phase transition again allowing one to study another mixed state. Our developed laser-induced thermoelectric mapping method hence confirms the presence of interfaces between two charge density phases in 1T-TaS₂.

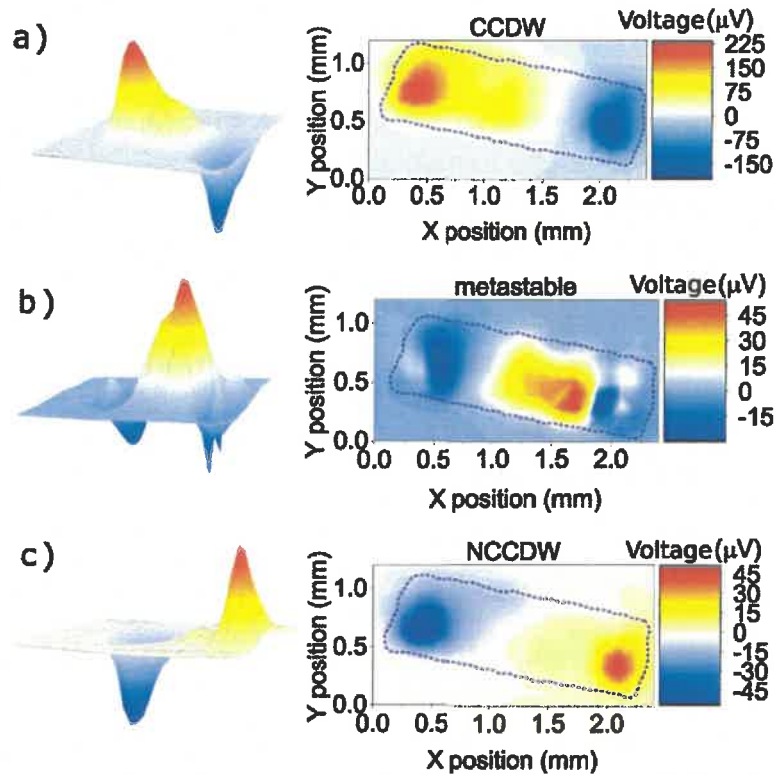


Figure 11: Laser-induced thermoelectric voltage maps obtained for (a) CCDW state at $T=140$ K, (b) metastable state of the sample during an interrupted NCCDW-CCDW phase transition at $T=215$ K, (c) NCCDW state at $T=230$ K.

In the publication [H6] we address another interface that may appear even within a single phase. We employed polarisation-resolved micro-Raman spectroscopy to study the symmetries of the observed Raman modes in the low-temperature CCDW phase. Our measurements showed that the point groups that were reported in the literature cannot explain the observed behaviour, most prominently the insusceptibility of the Raman signal to a rotation of the sample. An antisymmetric Raman tensor is needed to explain the observed behaviour. Such Raman tensors are also used to explain the effect of Raman optical activity for molecular light scattering, which allows to probe the chirality of molecules in biological mater [23]. The question of whether the charge density compound 1T-TaS₂ is chiral is difficult to assess. In contrast to standard measurements of optical activity, one cannot just

measure the transmitted polarisation, since the bulk material is opaque. In our work, we are able to show that one can use circularly polarised excitation and detection to measure the Raman optical activity of 1T-TaS₂. Figure 12 shows such results. One can observe three types of lines. The first set of lines is more intense for excitation with σ^+ and detection with σ^- . The second set of lines is more intense for the opposite excitation scheme and the third set of lines is not influenced at all. These signatures of different responses to circularly polarised light indicate that 1T-TaS₂ shows Raman optical activity and is indeed chiral, as opposed to previous results that did not report chirality in pristine samples [24, 25]. It is worth mentioning that our results were already reproduced by two independent groups that found the same Raman response [26, 27].

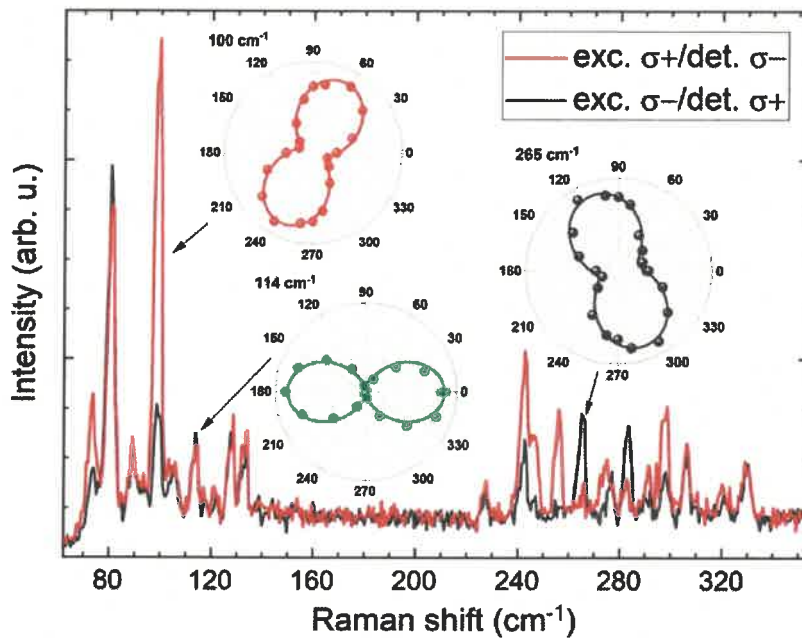


Figure 12: Raman scattering spectra of bulk 1T-TaS₂ obtained in circularly polarized light in σ^+/σ^- and σ^-/σ^+ configurations, where σ^+ (σ^-) means right-handed (left-handed) circularly polarized light, measured at $T=5$ K. The insets show angular plots of linear polarization of three lines, 100, 114, and 265 cm^{-1} .

Although not reported for the pristine CCDW state, signs of chirality were observed as intertwined chiral charge orders in scanning tunnelling microscopy images for a so called “hidden” state in 1T-TaS₂ [28]. Such hidden metastable states were observed in 1T-TaS₂ after pulsed laser excitation [29, 30]. More recent work shows that even an incoherent white light illumination can have a strong impact on 1T-TaS₂, leading to a change of stacking between CCDW supercells in consecutive layers [31]. We believe that by measuring Raman spectroscopy we influence the material within the laser spot, which may lead to an interface between the pristine area (dark region) and the modified area (within the laser spot). The illuminated area may show a different stacking and other properties similar to those in the case of the hidden state. The role of light illumination may play a fundamental role to describe the observed effects and it is clear that more work which combines different measurement techniques is needed to

understand the process involved in more detail. However, the results presented for 1T-TaS₂ suggest that interfaces induced by light exposure can also appear within a single phase of a single layered material.

The presented series of publications, dedicated to interfaces within and with other of layered materials, allowed us to study a broad range of phenomena that highlight not only the possibilities, but also the challenges when designing novel concepts based on van der Waals heterostructures. It was possible to unveil the following effects related to physical processes at interfaces:

- Tunnelling of charge carriers directly into excitonic states (sub-bandgap electroluminescence);
- Magneto-oscillations in the electroluminescence caused by Landau quantization in the graphene electrodes of vdW heterostructures;
- Formation, electrical pumping, and observation of interlayer excitons in vdW heterostructures;
- Upconversion of the electroluminescence via the Auger effect of interlayer excitons;
- Direct under-etching of 2D materials by photocorrosion of germanium;
- Quenching of the Raman signal for graphene on germanium;
- Radiolysis of interfacial water and hydrogen generation at the sapphire / hBN interface;
- Occurrence and mapping of metastable charge density wave states in 1T-TaS₂ by spatial maps of the Seebeck response;
- Light induced interfaces and chirality of 1T-TaS₂ as evidenced by the observation of Raman optical activity.

References:

- [1] Geim, A. and Grigorieva, I. *Nature* **499**(7459), 419–425 (2013).
- [2] Withers, F., Del Pozo-Zamudio, O., Mishchenko, A., Rooney, A. P., Gholinia, A., Watanabe, K., Taniguchi, T., Haigh, S. J., Geim, A. K., Tartakovskii, A. I., and Novoselov, K. S. *Nature Materials* **14**(3), 301–306 (2015).
- [3] He, K., Kumar, N., Zhao, L., Wang, Z., Mak, K. F., Zhao, H., and Shan, J. *Physical Review Letters* **113**(2), 026803 (2014).
- [4] Zhang, C., Chen, Y., Johnson, A., Li, M.-Y., Li, L.-J., Mende, P. C., Feenstra, R. M., and Shih, C.-K. *Nano Letters* **15**(10), 6494–6500 (2015).
- [5] Lee, J.-H., Lee, E. K., Joo, W.-J., Jang, Y., Kim, B.-S., Lim, J. Y., Choi, S.-H., Ahn, S. J., Ahn, J. R., Park, M.-H., et al. *Science* **344**(6181), 286–289 (2014).
- [6] Sitek, J., Pasternak, I., Grzonka, J., Sobieski, J., Judek, J., Dabrowski, P., Zdrojek, M., and Strupinski, W. *Applied Surface Science* **499**, 143913 (2020).
- [7] Persichetti, L., De Seta, M., Scaparro, A., Miseikis, V., Notargiacomo, A., Ruocco, A., Sgarlata, A., Fanfoni, M., Fabbri, F., Coletti, C., et al. *Applied Surface Science* **499**, 143923 (2020).

- [8] Ruberto, M. N., Zhang, X., Scarmozzino, R., Willner, A. E., Podlesnik, D. V., and Osgood, R. M. *Journal of The Electrochemical Society* **138**(4), 1174 (1991).
- [9] Paszkowicz, W., Pelka, J. B., Knapp, M., Szyszko, T., and Podsiadlo, S. *Applied Physics A* **75**(3), 431–435 (2002).
- [10] Iwanski, J., Tatarczak, P., Tokarczyk, M., Dabrowska, A. K., Pawlowski, J., Binder, J., Kowalski, G., Stepniewski, R., and Wysmolek, A. *Nanotechnology* **34**(1), 015202 (2022).
- [11] Veirs, D. K. and Rosenblatt, G. M. *Journal of molecular spectroscopy* **121**(2), 401–419 (1987).
- [12] Hu, S., Lozada-Hidalgo, M., Wang, F. C., Mishchenko, A., Schedin, F., Nair, R. R., Hill, E. W., Boukhvalov, D. W., Katsnelson, M. I., Dryfe, R. A. W., Grigorieva, I. V., Wu, H. A., and Geim, A. K. *Nature* **516**(7530), 227–230 (2014).
- [13] He, L., Wang, H., Chen, L., Wang, X., Xie, H., Jiang, C., Li, C., Elibol, K., Meyer, J., Watanabe, K., Taniguchi, T., Wu, Z., Wang, W., Ni, Z., Miao, X., Zhang, C., Zhang, D., Wang, H., and Xie, X. *Nature Communications* **10**(1), 2815 (2019).
- [14] Blundo, E., Surrente, A., Spirito, D., Pettinari, G., Yildirim, T., Chavarin, C. A., Baldassarre, L., Felici, M., and Polimeni, A. *Nano Lett.* **22**(4), 1525–1533 (2022).
- [15] Le Caër, S. *Water* **3**(1), 235–253 (2011).
- [16] Wilson, J., Salvo, F. D., and Mahajan, S. *Adv. Phys.* **24**(2), 117–201 (1975).
- [17] Ishiguro, T. and Sato, H. *Phys. Rev. B* **44**(5) 08 (1991).
- [18] Lutsyk, I., Rogala, M., Dabrowski, P., Krukowski, P., Kowalczyk, P. J., Busiakiewicz, A., Kowalczyk, D. A., Lacinska, E., Binder, J., Olszowska, N., Kopciuszynski, M., Szalowski, K., Gmitra, M., Stepniewski, R., Jalochocki, M., Kolodziej, J. J., Wysmolek, A., and Klusek, Z. *Phys. Rev. B* **98**, 195425 Nov (2018).
- [19] Dai, J., Calleja, E., Alldredge, J., Zhu, X., Li, L., Lu, W., Sun, Y., Wolf, T., Berger, H., and McElroy, K. *Phys. Rev. B* **89**, 165140 (2014).
- [20] Albertini, O., Zhao, R., McCann, R., Feng, S., Terrones, M., Freericks, J., Robinson, J., and Liu, A. *Physical Review B* **93** 11 (2015).
- [21] Suzuki, A., Yamamoto, R., Doyama, M., Mizubayashi, H., Okuda, S., Endo, K., and Gonda, S. *Solid State Commun.* **49**(12), 1173 – 1176 (1984).
- [22] Inada, Onuki, and Tanuma. *Physica B+C* **99** 01 (1980).
- [23] Barron, L. D. and Buckingham, A. D. *Annu. Rev. Phys. Chem.* **26**(1), 381–396 (1975).
- [24] Ishioka, J., Liu, Y. H., Shimatake, K., Kurosawa, T., Ichimura, K., Toda, Y., Oda, M., and Tanda, S. *Phys. Rev. Lett.* **105**, 176401 (2010).

- [25] Gao, J. J., Zhang, W. H., Si, J. G., Luo, X., Yan, J., Jiang, Z. Z., Wang, W., Lv, H. Y., Tong, P., Song, W. H., Zhu, X. B., Lu, W. J., Yin, Y., and Sun, Y. P. *Appl. Phys. Lett.* **118**(21), 213105 (2021).
- [26] Yang, H. F., He, K. Y., Koo, J., Shen, S. W., Zhang, S. H., Liu, G., Liu, Y. Z., Chen, C., Liang, A. J., Huang, K., Wang, M. X., Gao, J. J., Luo, X., Yang, L. X., Liu, J. P., Sun, Y. P., Yan, S. C., Yan, B. H., Chen, Y. L., Xi, X., and Liu, Z. K. *Phys. Rev. Lett.* **129**, 156401 (2022).
- [27] Zhao, Y., Nie, Z., Hong, H., Qiu, X., Han, S., Yu, Y., Liu, M., Qiu, X., Liu, K., Meng, S., Tong, L., and Zhang, J. *Nature Communications* **14**(1), 2223 (2023).
- [28] Gerasimenko, Y. A., Karpov, P., Vaskivskiy, I., Brazovskii, S., and Mihailovic, D. *npj Quantum Materials* **4**(1), 32 (2019).
- [29] Stojchevska, L., Vaskivskiy, I., Mertelj, T., Kusar, P., Svetin, D., Brazovskii, S., and Mihailovic, D. *Science* **344**(6180), 177–180 (2014).
- [30] Vaskivskiy, I., Gospodaric, J., Brazovskii, S., Svetin, D., Sutar, P., Goreshnik, E., Mihailovic, I. A., Mertelj, T., and Mihailovic, D. *Sci. Adv.* **1**(6) (2015).
- [31] Li, W. and Naik, G. V. *Nano Lett.* **20**(11), 7868–7873 (2020).

5. Presentation of significant scientific or artistic activity carried out at more than one university, scientific or cultural institution, especially at foreign institutions

Before PhD degree

Before obtaining the PhD degree, I was scientifically active at the following four Universities:

i. University of Tübingen, Germany (MSc thesis)

I obtained my MSc degree at the Faculty of Applied Physics at the University of Tübingen in the group of prof. Dieter Klein. My activity was mostly concentrated on semiconductor processing techniques (clean room facilities), carbon nanotube growth by Plasma Enhanced Chemical Vapour Deposition (PECVD), and measurements of field emission currents in Ultra-high vacuum (UHV).

ii. Faculty of Physics, University of Warsaw, Poland (PhD thesis)

After obtaining my MSc degree in Tübingen I was awarded a scholarship in the framework of the “International PhD projects (MPD)” of the Foundation for Polish Science. My work focused on GaN and graphene for possible future sensing applications.

iii. Australian National University, Canberra, Australia (5 months)

During my research stay in Canberra in the framework of the “International PhD projects (MPD)” of the Foundation for Polish Science, I worked on ion implantation of carbon in GaN HEMT structures to form insulating channels and the ion implantation of nitrogen into SiC covered by graphene (epitaxial samples) to obtain n-doped areas. The latter experiments allowed to fabricate a buried gate that enabled to tune the charge carrier concentration in graphene as evidenced by changes in the Shubnikov-de Haas oscillations measured in Warsaw. These results became part of my PhD thesis.

- iv. *French National High Magnetic Field Laboratory, Grenoble, France (3 months)*
During my first research stay in Grenoble I performed magneto-Raman experiments of graphene flakes naturally occurring on graphite. The obtained results became part of my PhD thesis and were published in two articles (EPL and 2D Materials).

After PhD degree

After obtaining my PhD degree, I took on a position as post-doctoral researcher at the CNRS in Grenoble

- *Post-doctoral position - French National High Magnetic Field Laboratory, Grenoble, France (12 months)*
From May 2015 until the end of April 2016 I was part of the group of prof. Marek Potemski holding a position financed by the Graphene Flagship programme of the European Union. During my stay I worked mainly on the electroluminescence of novel van der Waals heterostructures in collaboration with the group of Nobel prize laureate prof. Konstantin Novoselov from the University of Manchester. During this time I observed many novel effects, which are described in more detail in point 4 and the publications [H1] and [H2].

Research visits

- Laboratoire Charles Coulomb, CNRS, Montpellier, France
Research group: prof. Guillaume Cassabois, prof. Bernard Gil
Period of stay: 13.2-18.2.2022
Optical measurements of our hexagonal boron nitride samples in the deep UV range
- French National High Magnetic Field Laboratory, CNRS, Grenoble, France
Research group: prof. Marek Potemski
Period of stay: 25.06.2017- 02.07.2017
Measurements of the photoluminescence and electroluminescence of van der Waals heterostructures together with members of the group of prof. Novoselov

- French National High Magnetic Field Laboratory, CNRS, Grenoble, France
 Research group: prof. Marek Potemski
 Period of stay: 12.2.2017- 25.2.2017
Measurements of the photoluminescence and electroluminescence of van der Waals heterostructures together with members of the group of prof. Novoselov

6. Presentation of teaching and organizational achievements as well as achievements in popularization of science or art.

The list of achievements below corresponds to the time period from 2016 (adiunkt position at the University of Warsaw)

Teaching

Lectures:

Second cycle studies:

- Introduction to optics and condensed matter physics (condensed matter physics part)
- Forensic physicochemistry (Electron microscopy in forensic science, Raman spectroscopy and luminescence)

Classes:

First cycle studies:

- Physics with Mathematics I, exercises

Second cycle studies:

- Introduction to optics and condensed matter physics (condensed matter physics part)
- Low-dimensional systems and nanostructures

Laboratory courses:

First cycle studies:

- Laboratory of Measurement Techniques and Electronics

Second cycle studies:

- Physical and chemical analysis of substances
- Physics Laboratory, 2nd Level
- Advanced Laboratory for Nanostructure Engineering
- III Laboratory (Semiconductors)
- Individual Preliminary Laboratory

Experimental demonstrations for lectures:

First cycle studies:

- Fundamentals of Physics IV
- Thermodynamics with Elements of Statistical Physics

Other:

Second cycle studies:

- Semiconductor physics - students seminar (supervision of students)
- Post-graduate internship in our laboratory

Supervision of PhD, MSc and BSc theses

PhD theses (co-supervisor):

1. Jakub Kierdaszuk: *"Investigation of scattering processes in graphene on nanowires substrate"* (date of PhD award: 07.02.2022)
2. Ewa Łacińska: *"Impact of Phase Transitions on Optical and Electrical Properties of 1T-TaS₂"* (date of PhD defence: 04.07.2023)
3. Piotr Kaźmierczak: *"Modification of properties of graphene structures and generation of electrical signals under the influence of flow of aqueous solutions"* (in progress)
4. Katarzyna Ludwiczak: *"Novel epitaxial 2D heterostructures: towards wafer scale"* (in progress)
5. Jakub Rogoża: *"Epitaxial boron nitride - a platform for deep ultraviolet light detectors and emitters"* (in progress)
6. Piotr Tatarczak: *"Single photon emitters and optical microcavities based on epitaxial boron nitride - a new approach"* (in progress)

MSc theses:

1. Batrosz Danilewicz: *Raman spectroscopy of automotive paints (in progress)*
2. Leonid Tkachenko: *Analysis of the surface morphology of epitaxial hexagonal boron nitride layers by computer vision (2021)*
co-supervisor: dr hab. Artur Kalinowski, prof. UW
3. Emma Grodzicka: *Single photon emission in epitaxial hexagonal boron nitride (2020)*
4. Katarzyna Ludwiczak: *Optical studies and passivation of selected layered materials (2020)*

5. Katarzyna Konieczna: *Study of gunshot residue using Raman spectroscopy* (2020)
6. Jakub Rogoża: *Raman spectroscopy studies of graphene grown on germanium and fabrication of graphene membranes via photocorrosion* (2020), co-supervisor: prof. Andrzej Wyszomolek
7. Maksymilian Wojtczak: *Substrates for gating 2D materials using boron nitride / boron carbide structures grown by MOVPE* (2020) co-supervisor: prof. Andrzej Wyszomolek

BSc theses:

1. Katarzyna Ludwiczak: *Electrooptical study of phase transitions in TaS₂* (2019)
2. Maksymilian Wojtczak: *Optical and electrical characterization of doped boron nitride epitaxial layers* (2019), co-supervisor: prof. Andrzej Wyszomolek
3. Katarzyna Rogoża: *Investigation of graphene flakes and its derivatives* (2017) co-supervisor: prof. Andrzej Wyszomolek

Popularization of science

- Press releases:
 - *Exciting Optoelectronic Properties Of Stacks Of Two-Dimensional Crystals*, Faculty of Physics, University of Warsaw (16.9.2019)
<https://www.photoniconline.com/doc/exciting-optoelectronic-properties-of-stacks-of-two-dimensional-crystals-0001>
 - *Manchester researchers demonstrate low voltage LEDs*, University of Manchester (1.8.2019)
<https://www.manchester.ac.uk/discover/news/manchester-researchers-demonstrate-low-voltage-leds/>
- Radio Kampus: Interview on the subject of the Nature Communications publication: "Upconverted electroluminescence via Auger scattering of interlayer excitons in van der Waals heterostructures", 25.6.2019
- Workshop: „With a laser into a 2D crystal”, Open day at the Ochota Campus 2018
- Workshop: „With a laser into graphene and other 2D materials”, Open day at the Ochota Campus 2017

Organizational achievements

- Head of the lithography laboratory and cleanroom facilities:
 - Commissioning and management of infrastructure of the Solid State Physics Division of the Faculty of Physics in the CeNT I building
 - Management of the related SPUB grant
- Chairman of the International School of Semiconductors in the framework of the „Jaszowiec International School & Conference on the Physics of Semiconductors”. Member of the program and organizing committee. Editions:
 - 49th “Jaszowiec 2021”, 1.9.-10.9.2021
 - 48th “Jaszowiec 2019”, 8.6.-14.6.2019
- Member of the Faculty Council (Rada Wydziału) (11.2016 – present)

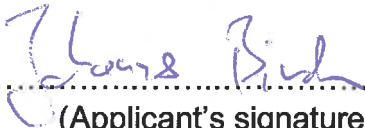
7. Apart from information set out in 1-6 above, the applicant may include other information about his/her professional career, which he/she deems important

Awards

- Outstanding reviewer award 2021 for the journal: 2D Materials
- “IOP Trusted reviewer” award (2020)
- Team award for scientific achievements by the Rector of the University of Warsaw (2022)
- Individual award for scientific achievements (III degree) by the Rector of the University of Warsaw (2017)

Scholarships

- 2010-2014 – PhD scholarship within the framework of the “International PhD projects” (MPD) of the Foundation for Polish Science (FNP) co-financed by the EU European Regional Development Fund
- Scholarship of the Polish Government


.....
(Applicant's signature)

